

UC Berkeley

UC Berkeley Previously Published Works

Title

High intensity focused ultrasound as a tool for tissue engineering: Application to cartilage

Permalink

<https://escholarship.org/uc/item/56z0x6fg>

Journal

Medical Engineering & Physics, 38(2)

ISSN

1350-4533

Authors

Nover, Adam B
Hou, Gary Y
Han, Yang
et al.

Publication Date

2016-02-01

DOI

10.1016/j.medengphy.2015.11.016

Peer reviewed



Published in final edited form as:

Med Eng Phys. 2016 February ; 38(2): 192–198. doi:10.1016/j.medengphy.2015.11.016.

High Intensity Focused Ultrasound as a Tool for Tissue Engineering: Application to Cartilage

Adam B. Nover^a, Gary Y. Hou^a, Yang Han^a, Shutao Wang^a, Grace D. O'Connell^{a,b}, Gerard A. Ateshian^{a,c}, Elisa E. Konofagou^{a,d}, and Clark T. Hung^a

Adam B. Nover: abn2106@columbia.edu; Gary Y. Hou: yh2367@columbia.edu; Yang Han: yh2583@columbia.edu; Shutao Wang: sw2735@columbia.edu; Grace D. O'Connell: g.oconnell@berkeley.edu; Gerard A. Ateshian: ateshian@columbia.edu; Elisa E. Konofagou: ek2191@columbia.edu; Clark T. Hung: cth6@columbia.edu

^aDepartment of Biomedical Engineering, Columbia University, 351 Engineering Terrace, 1210 Amsterdam Avenue, Mail Code: 8904, New York, NY 10027, USA

^bDepartment of Mechanical Engineering, University of California Berkeley, 5122 Etcheverry Hall, Mailstop 1740, Berkeley, CA 94720-1740, USA

^cDepartment of Mechanical Engineering, Columbia University, 242 S. W. Mudd, 500 West 120th Street, Mail Code: 4703, New York, NY 10027, USA

^dDepartment of Radiology, Columbia University, 630 W. 168th St., P&S Box 28, New York, NY 10032, USA

Abstract

This article promotes the use of High Intensity Focused Ultrasound (HIFU) as a tool for affecting the local properties of tissue engineered constructs *in vitro*. HIFU is a low cost, non-invasive technique used for eliciting focal thermal elevations at variable depths within tissues. HIFU can be used to denature proteins within constructs, leading to decreased permeability and potentially increased local stiffness. Adverse cell viability effects remain restricted to the affected area. The methods described in this article are explored through the scope of articular cartilage tissue engineering and the fabrication of osteochondral constructs, but may be applied to the engineering of a variety of different tissues.

Corresponding Author: Clark T. Hung, ; Email: cth6@columbia.edu, Department of Biomedical Engineering, Columbia University, 351 Engineering Terrace MC: 8904, 1210 Amsterdam Avenue, New York, NY, 10027, USA, Phone: +1 212-854-6542, Fax: +1 212-854-8725.

Research was performed at the Cellular Engineering Laboratory and the Ultrasound Elasticity Imaging Laboratory at Columbia University, New York, NY, USA.

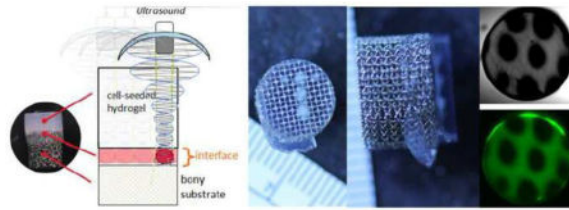
Author Contributions: All authors contributed significantly to the work reported in this manuscript. ABN, GDO, EEK, and CTH designed the experiments. ABN, GYH, YH, and SW carried out the experiments and collected the data. ABN, GYH, YH, SW, EEK, and CTH analyzed the data. GDO, GAA, EEK, and CTH supervised and advised the work. ABN, EEK, and CTH wrote the paper. All authors have read and approved the final submitted manuscript.

Disclosures

Titanium bases provided by Stryker Orthopaedics (Mahwah, NJ, USA). No competing financial interests exist. All authors contributed to the conception and design of the study, collection and analysis of data, drafting and revising the manuscript, and gave final approval of this submitted work.

Publisher's Disclaimer: This is a PDF file of an unedited manuscript that has been accepted for publication. As a service to our customers we are providing this early version of the manuscript. The manuscript will undergo copyediting, typesetting, and review of the resulting proof before it is published in its final citable form. Please note that during the production process errors may be discovered which could affect the content, and all legal disclaimers that apply to the journal pertain.

Graphical abstract



Keywords

tissue engineering; high intensity focused ultrasound (HIFU); articular cartilage; osteochondral grafts

Introduction

In the field of tissue engineering there exists a need to generate tissues with specific local tissue properties so to match native tissue architecture and therefore gain true functionality. For example, engineered osteochondral grafts [1, 2] are being investigated as an alternative to osteochondral allografts, which are of scarce supply [3, 4]. Native tissue contains a mineralized subchondral plate, which anchors mature cartilage, separating it from the underlying vascularized bone, providing a virtually impermeable interface. This subchondral interface promotes the elevated interstitial fluid pressurization needed for load-bearing and lubrication mechanisms in articular cartilage [5–9]. However, engineered osteochondral tissues, consisting of a chondrocyte-seeded hydrogel atop a nonliving porous, bone-like substrate, lack any sort of subchondral plate *a priori*. Incorporation of such an impermeable layer from the start, such as via a denser porosity region in the bony substrate localized to the gel-substrate overlap region [10], would block nutrient transport across the layer during tissue culture. Since nutrient transport is critical for the development of engineered tissue [11, 12], a technology is required that can stiffen or seal the bone-cartilage interface at an optimal time during *in vitro* growth.

High intensity focused ultrasound (HIFU) may offer such an ability. Like other forms of ultrasound, HIFU is a minimally or non-invasive, non-contact, non-radiation, low-cost technology. It is under investigation for its use in soft-tissue cancer therapy [13] and is currently FDA approved for uterine fibroid ablation [14, 15]. HIFU can penetrate depths of at least 10 cm and reach temperatures of at least 80°C [16, 17]. Studies have shown that HIFU's thermal and mechanical effects can lead to a loss of *in vitro* viability [18], yet the thermal effects of HIFU remain the primary mechanism of damage [16] and repair tissues enter the periphery of the treated region after two weeks [17].

In conjunction with heat, an additional substance may be necessary for inducing a change in tissue properties. Heat-induced protein denaturation has been demonstrated in a number of tissues and protein-incorporated gel phantoms, often leading to color change, coagulation, and, after certain temperatures, irreversible stiffening [19–27]. Albumin is commonly used in gel phantoms for tissue ablation studies via thermal treatment modalities, such as HIFU

[23–26, 28]. Albumin from bovine serum (BSA) or egg white, a more economical option, coagulates at $67\pm 1^\circ\text{C}$ via intermolecular β -sheet formation, changing from a clear color to an opaque white, providing easy visualization of the heated region [20, 24]. Outside of phantoms, albumin has been utilized as a biological solder [29]. With respect to articular cartilage, albumin is relevant; it is the chief protein component of synovial fluid [30]. For these reasons, the addition of albumin may aid the alteration of internal properties of tissue engineered constructs, especially prior to cellular protein elaboration.

While most research utilizing HIFU technology aims to induce pressures and/or thermal elevation over large (cm scale) areas of dense tissue *in vivo*, such as in full tumor ablation, here HIFU is investigated as a potential tool for precisely modulating the spatial properties of small (mm scale) tissue engineered constructs during *in vitro* growth, which increase in density during culture (agarose gel scaffold is 98% w/v water on initial seeding day). Here, the aim of this study is to test the feasibility of HIFU as a method of altering local tissue properties as a tool for tissue engineering, namely forming a biomimetic subchondral plate in engineered osteochondral constructs by thermally affecting the interface region.

Methods

HIFU Setup

HIFU treatment was conducted according to [27], utilizing a setup conducive to later incorporation of Harmonic Motion Imaging (HMI), an ultrasound-based method of monitoring elastographic changes in tissues [27, 31–33]. Briefly, this setup consists of an imaging transducer centrally positioned inside a confocal therapeutic transducer (Fig. 1A) and attached to a computer-controlled positioner (Velmex Inc. Bloomfield, NY, USA). The two transducers were self-contained by attaching to a coupling cone containing degassed, distilled water and sealed with an acoustically transparent latex membrane [34, 35], which allows the membrane to be coupled to the sample through degassed culture media, phosphate buffered saline (PBS), water, or ultrasound gel. For imaging, a 7.5 MHz single-element pulse-echo transducer (Panametrics, Waltham, MA, USA) connected to a pulser/receiver (Panametrics 5051PR or Olympus 5072PR, Waltham, MA, USA) was used to target and monitor treatment produced by the therapeutic transducer. For thermal treatment, either a 4.755 MHz (Riverside Research Institute, New York, NY, USA) or a 4.5 MHz (Imasonics, Besancon, France) therapeutic transducer was used. Heating parameters vary; these parameters represent an aspect of this treatment which will require further optimization. Two function generators (Agilent (HP) 33120 A and 33220A, Palo Alto, CA, USA) were used to drive the therapeutic transducer with an amplitude-modulated waveform, combining sine waves: one of the therapeutic transducer's excitation frequency at a varied amplitude with a 25 Hz wave of amplitude $5.086 V_{\text{peak-to-peak}}$. The signal was then amplified by 50 dB using a power amplifier. For HIFU treatment, constructs or cell-seeded slabs were submerged in degassed PBS or culture media.

Gel Construct Fabrication and Media Formulation

As in our previous cartilage tissue engineering studies, gels were cast with final concentrations of 2% w/v agarose (Type VII or IX-A, Sigma-Aldrich, St. Louis, MO, USA)

and 30 million cells/mL as gel-alone or osteochondral constructs according to [1]. In studies where albumin was incorporated, equal volumes of egg white and 120 million cells/mL solution were mixed, then equal volumes of that solution and 4% w/v agarose were mixed, yielding gels of 30 million cells/mL, 2% w/v agarose, and 25% v/v egg white. In acellular studies, cell solutions were replaced with PBS (Sigma-Aldrich). Passaged chondrocytes enzymatically isolated from juvenile bovine calf carpometacarpal or knee joints were used for all studies [36, 37].

Dulbecco's Modified Eagle's Medium (DMEM, Invitrogen, Carlsbad, CA, USA) with 10% fetal bovine serum (FBS, Atlanta Biologics, Atlanta, GA, USA), 10 ng/mL PDGF, 1 ng/mL TGF- β 1 (Invitrogen), 5 ng/mL FGF-2 (Invitrogen), and 1% antibiotic-antimycotic (Invitrogen) was used for all instances of passaging [37]. Constructs were cultured in chondrogenic media (CM), consisting of DMEM with 50 μ g/mL L-proline (Sigma-Aldrich), 100 μ g/mL sodium pyruvate (Sigma-Aldrich), 1% ITS+ premix (BD Biosciences, Franklin Lakes, NJ, USA), 100 nM dexamethasone (Sigma-Aldrich), 1% antibiotic-antimycotic, and 50 μ g/mL ascorbic acid (Sigma-Aldrich) [37].

Spatiotemporal Control of HIFU/Power Optimization

An example of irreversible, heat-induced protein denaturation and stiffening in a gel phantom is displayed and described in Fig. 1B–C.

Controlled patterning of thermally affected regions were induced in acellular, albumin-containing agarose (Type VII) phantoms by moving a therapeutic transducer in a 2D raster-scan fashion.

Thermally affected regions were produced at various powers and durations on acellular, albumin-containing osteochondral constructs (agarose Type VII) cast atop ϕ 10 mm titanium disks (Stryker Orthopaedics, Mahwah, NJ, USA). The lowest combination inducing consistent albumin color change was selected for subsequent osteochondral interface heating studies.

Albumin Incorporation in Engineered Constructs

Passage 2 juvenile bovine chondrocyte-seeded constructs were cast using Type IX-A agarose creating the following groups: control samples (without albumin); egg white-containing constructs; and 5% w/v BSA (cast by mixing equal volumes of 120×10^6 cells/mL suspension and 20% w/v BSA in PBS, then mixing equal volumes of this solution with 4% w/v agarose). For the duration of a 28-day period, constructs were mechanically tested in unconfined compression (G^* , dynamic modulus at 0.5 Hz) [6]. Constructs were lyophilized, weighed dry (DW), and then digested in 0.5 mg/mL proteinase K (MP Biomedicals, Santa Ana, CA, USA) for 16 h at 50 °C. Glycosaminoglycan (GAG) content was quantified with a 1,9-dimethylmethylene blue (Sigma-Aldrich) dye-binding assay [38].

Post-HIFU effects on Solute Transport

An acellular albumin-containing gel (agarose Type VII) slab of thickness 2.3 mm was cast, pinned across rubber stoppers, and placed in a degassed PBS/1% antibiotic-antimycotic

solution. HIFU was applied using 11.6 W total acoustic power in a raster pattern to induce thermally affected focal regions across a 14×14 mm square plane of the gel (15×15 points, 10 s/point). Cylinders ($\phi 3$ mm) were punched from affected gel region. Disks were washed twice with PBS/10% antibiotic-antimycotic solution, then soaked in a saturated 0.5 mg/mL 70 kDa fluorescein-conjugated dextran (Invitrogen) solution, and then imaged using a confocal microscope (Olympus Fluoview FV1000, Waltham MA, USA).

Temperature Measurement during HIFU Application

To gain an appreciation for the local heating temperatures associated with HIFU application, thermocouple studies were performed on acellular egg white-containing agarose (Type VII) gels cast on $\phi 10$ mm titanium bases (gel-bony substrate) or as two layered slabs (gel-gel). A 40-gauge T-type bare wire thermocouple (Philips Research North America, Briarcliff Manor, NY, USA) was placed into gel towards the osteochondral interface or between two layered slabs [39]. The thermocouple was targeted by inducing low power heating for 2 s per point in a raster fashion, then moving toward the point of highest temperature rise (performed in the x-, y-, and z-directions). Temperature data was recorded for 60 s including a 20 s application of 0.56 W or 11.6 W total acoustic power on three osteochondral constructs and in three different locations between the layered slabs (n=3).

Viability & Culture of Cell-Seeded Gel Constructs after HIFU

To assess cell viability effects, an albumin-containing cellular agarose (Type VII) slab of 2.3 mm thickness was placed on a silicon rubber/absorber over polyurethane foam within a 100 mm culture dish and immersed in phosphate buffered saline. A 4.5 MHz HIFU transducer was used at ~ 5.9 W total acoustic power (excitation time: 3 s/point) to raster thermally affected regions into the slab. The transducer's focus was aimed towards the bottom of the slab. The slab was punched in thermally treated and untreated (control) areas using a 4 mm biopsy punch; thermally affected regions were kept within each disk. For 6 weeks, constructs were maintained with CM, changed every 2–3 days. Parallel samples from each group were halved, stained with Live/Dead Kit (Invitrogen), and imaged using a confocal microscope (Leica TCS SP5, Wetzlar, Germany) with n=1 sample per n=4 time points.

As a more robust follow-up, Passage 4 juvenile bovine chondrocytes were cast in agarose (Type VII) with albumin on porous titanium bases of 4 and 10 mm diameter, with a gel thickness of ~ 2 mm. To maintain sterility, constructs were sterilely placed in a custom apparatus with degassed CM, and half were subjected to HIFU treatment. The custom apparatus uses an acoustically transparent polydimethylsiloxane (PDMS) membrane to separate constructs in sterile, degassed CM, from a reservoir of non-sterile degassed, distilled water to which the HIFU system is acoustically coupled. The 10 mm osteochondral constructs were thermally affected in a 3 X 3 pattern and 4 mm osteochondral constructs were thermally affected at a single point using a power of 11.6 W total acoustic power for a 20 s duration. Following treatment, constructs were removed from the device in a sterile hood, transferred to culture dishes, and cultured for 28 days in CM with 14 days of 10 ng/mL TGF- $\beta 3$ supplementation [40]. On days 0 and 28, constructs were evaluated for GAG content as described above. Cell viability was assessed with a Live/Dead stain imaged on a confocal microscope (Olympus Fluoview FV1000).

Statistical Analyses

Statistica (Statsoft, Tulsa, OK, USA) was used to perform one-way analysis of variance (ANOVA) tests followed by Tukey's honest significant difference (HSD) post-hoc test ($\alpha=0.05$) to determine statistical significance ($p < 0.05$). Microsoft Excel (Redmond, WA, USA) was utilized to calculate the 95% confidence interval (CI) of group means and differences between means. Data is displayed as mean \pm 95% CI.

Results

Spatiotemporal Control of HIFU/Power Optimization

HIFU treatment could be induced at variable depths below the gel surface (Fig. 1D), and formed into patterns based on the movement of the transducer and the duration of the treatment. On porous titanium bases, 20 s of treatment at 11.6 W total acoustic power was found to reliably produce a visible thermally affected region (Fig. 1E).

Albumin Incorporation in Engineered Constructs

Albumin-containing constructs grew to a similar extent as the controls (Fig. 2). Compared to the control's G^* , the mean difference was 0.24 ± 0.34 MPa for egg white-containing constructs and 0.31 ± 0.29 MPa for BSA-containing constructs. Compared to the control's GAG content per dry weight (g/g), the mean difference was 0.04 ± 0.03 for egg white-containing constructs and 0.02 ± 0.03 for BSA-containing constructs.

Post-HIFU effects on Solute Transport

Fluorescence images of the constructs soaked in fluorescein-labeled dextran showed uniform distribution of solute except for regions of rasterized thermally affected regions that appeared dark where dextran was excluded (Fig. 3A). These dark regions corresponded to those visualized by albumin color-change in transmitted light images.

Temperature Measurement during HIFU Application

With the application of 0.56 W total acoustic power, temperatures recorded at the gel-metal interface were in the 26–40 °C range while those between the stacked gel layers were between 23–25 °C (data not shown). With 11.6 W total acoustic power, the gel-metal temperatures were 80–100°C, while the layered gel temperatures were 30–45°C (Fig. 4).

Viability & Culture of Cell-Seeded Gel Constructs after HIFU

Immediately after the ultrasonic treatment, the thermally affected constructs contained a region of cell death (ethidium homodimer-1 staining, red; Fig. 5A), which corresponded with the white regions of heated albumin. The surrounding regions remained viable (calcein-AM staining, green). Control constructs remained viable throughout. Over the six week period, the cell death region remained localized, with some spots of viability appearing in the dead zone.

In the follow-up study, osteochondral constructs remained sterile following HIFU treatment. Fig. 3B shows the sterile chamber and the egg white lesion induced in osteochondral

constructs. Treatment was verified with the Live/Dead stain, showing dead regions which remained localized for 28 days in culture (Fig. 5B) confirming previous results. On day 0, GAG/DW (g/g) was 0.07 ± 0.019 (n=6) and 0.06 ± 0.003 (n=3) for 4 mm and 10 mm diameter constructs respectively. On day 28, this value increased to 0.23 ± 0.045 (n=7) and 0.24 ± 0.049 (n=4) for 4 mm and 10 mm diameter untreated constructs respectively. HIFU constructs showed similar GAG levels (4 mm: n=7; 10 mm: n=4); the differences in means between HIFU-treated constructs and untreated controls were 0.02 ± 0.07 and 0.04 ± 0.08 for 4 mm and 10 mm diameter constructs respectively. These studies repeat the incorporation of albumin without negative biocompatibility effects.

Discussion

HIFU is a unique method for applying thermal heating to local tissue regions and at various depths. Here we show that this technology can be applied to hydrogels used in tissue engineering. Incorporation of albumin can easily be incorporated upon initial gel fabrication, allowing for on-demand heat-induced denaturation without affecting tissue growth. Here we also show that this denaturation can block transport.

This internal reorganization of the egg white-gel scaffold can be utilized in tissue engineering, such as in the example of replicating a subchondral plate, a stiff, impermeable surface between cartilage and bone. This effect may also be delivered by other incorporable proteins. While this limited transport and increased stiffness may be desirable in a final tissue engineered product, these conditions would impede the *in vitro* development of the tissue by limiting nutrient transport to cells elaborating extracellular matrix. The depth penetrating aspects of ultrasound overcome this challenge by allowing for sterile on-demand treatment during *in vitro* tissue growth, ideally after a user predetermined amount of tissue development.

Treating tissues with heat is not unprecedented. In orthopaedics, radiofrequency probes and lasers have been utilized in the clinic, however both techniques are associated with cell death [41–45]. Here we show that the concomitant cell death of HIFU treatment remains localized over time with potential areas of recovery, which is reminiscent of the ability of engineered cartilage to recover after mechanical injury [36]. However, if recovery is poor, further extracellular matrix elaboration in the HIFU-treated area may be hindered. This suggests that this undesired effect could potentially be balanced against the intended changes in tissue properties.

From a therapeutic ultrasound perspective, one of the fascinating aspects of these studies is that these temperature elevations are induced in small, thin, non-dense materials. As ultrasound energy is deposited where mismatches in impedance occur, abutting materials can be used to assist the heating. Temperature measurements demonstrate this effect, showing that at the same powers, temperatures induced at a gel-metal interface is much greater than those at a gel-gel interface. In the case of introducing changes at an interface, this is quite beneficial.

To aid benchtop HIFU application, a custom chamber was fabricated to hold constructs (Fig. 3B, top). It can be sterilized and filled with media, degassed for ultrasound purposes. A thin membrane, which separates the sterile and non-sterile environments, remains invisible to ultrasound, allowing for the beam to travel through it. When tested, this concept allowed for ultrasonic treatment, maintenance of viable cells as confirmed by live/dead staining and subsequent *in vitro* growth.

HIFU treatment will require further optimization in order to realize its full potential for tissue engineering applications. The appropriate power level related to temperature elevation and duration as well as the timing of the treatment will vary for different tissues and applications. The effects of heating on cell matrix elaborated products may provide different effects in conjunction with those due to heating the gel scaffold and egg white. Also, additional research is required to determine how HIFU treatment modulates interface strength. On balance with the encouraging data that has been presented herein, HIFU appears to be a feasible tool for invoking changes in internal tissue properties on a concentrated, localized scale. As HIFU is already used clinically, it is conceivable that HIFU can also serve as a tool for additional regenerative medicine strategies *in situ*. We anticipate that HIFU will become a useful instrument in the field of tissue engineering research.

Acknowledgments

Research reported in this publication was supported by the National Institute of Arthritis and Musculoskeletal and Skin Diseases of the National Institutes of Health 2R01AR46568, National Institutes of Health R21EB014382, 1R01AR060361, and National Institute of Biomedical Imaging and Bioengineering of the National Institutes of Health 5P41EB002520. The content is solely the responsibility of the authors and does not necessarily represent the official views of the National Institutes of Health.

References

1. Nover AB, Lee SL, Georgescu MS, Howard DR, Saunders RA, Yu WT, et al. Porous Titanium Bases for Osteochondral Tissue Engineering. *Acta Biomater.* 2015
2. Lima EG, Chao PHG, Ateshian GA, Bal BS, Cook JL, Vunjak-Novakovic G, et al. The effect of devitalized trabecular bone on the formation of osteochondral tissue-engineered constructs. *Biomaterials.* 2008; 29:4292–9. [PubMed: 18718655]
3. Paige KT, Vacanti CA. Engineering new tissue: formation of neo-cartilage. *Tissue Eng.* 1995; 1:97–106. [PubMed: 19877919]
4. Mow VC, Ratcliffe A, Rosenwasser MP, Buckwalter JA. Experimental studies on repair of large osteochondral defects at a high weight bearing area of the knee joint: a tissue engineering study. *J Biomech Eng.* 1991; 113:198–207. [PubMed: 1875694]
5. Hwang J, Bae WC, Shieu W, Lewis CW, Bugbee WD, Sah RL. Increased hydraulic conductance of human articular cartilage and subchondral bone plate with progression of osteoarthritis. *Arthritis and rheumatism.* 2008; 58:3831–42. [PubMed: 19035476]
6. Soltz MA, Ateshian GA. Experimental verification and theoretical prediction of cartilage interstitial fluid pressurization at an impermeable contact interface in confined compression. *J Biomech.* 1998; 31:927–34. [PubMed: 9840758]
7. Park S, Krishnan R, Nicoll SB, Ateshian GA. Cartilage interstitial fluid load support in unconfined compression. *J Biomech.* 2003; 36:1785–96. [PubMed: 14614932]
8. Krishnan R, Kopacz M, Ateshian GA. Experimental verification of the role of interstitial fluid pressurization in cartilage lubrication. *Journal of orthopaedic research : official publication of the Orthopaedic Research Society.* 2004; 22:565–70. [PubMed: 15099636]

9. Pan J, Zhou X, Li W, Novotny JE, Doty SB, Wang L. In situ measurement of transport between subchondral bone and articular cartilage. *Journal of Orthopaedic Research*. 2009; 27:1347–52. [PubMed: 19360842]
10. Sherwood JK, Riley SL, Palazzolo R, Brown SC, Monkhouse DC, Coates M, et al. A three-dimensional osteochondral composite scaffold for articular cartilage repair. *Biomaterials*. 2002; 23:4739–51. [PubMed: 12361612]
11. Bian L, Angione SL, Ng KW, Lima EG, Williams DY, Mao DQ, et al. Influence of decreasing nutrient path length on the development of engineered cartilage. *Osteoarthritis and cartilage / OARS, Osteoarthritis Research Society*. 2009; 17:677–85.
12. Leddy HA, Awad HA, Guilak F. Molecular diffusion in tissue-engineered cartilage constructs: effects of scaffold material, time, and culture conditions. *J Biomed Mater Res B Appl Biomater*. 2004; 70:397–406. [PubMed: 15264325]
13. Fischer K, Gedroyc W, Jolesz FA. Focused ultrasound as a local therapy for liver cancer. *Cancer J*. 2010; 16:118–24. [PubMed: 20404608]
14. Hesley GK, Gorny KR, Henrichsen TL, Woodrum DA, Brown DL. A clinical review of focused ultrasound ablation with magnetic resonance guidance: an option for treating uterine fibroids. *Ultrasound Q*. 2008; 24:131–9. [PubMed: 18528271]
15. Stewart EA, Gedroyc WM, Tempany CM, Quade BJ, Inbar Y, Ehrenstein T, et al. Focused ultrasound treatment of uterine fibroid tumors: safety and feasibility of a noninvasive thermoablative technique. *Am J Obstet Gynecol*. 2003; 189:48–54. [PubMed: 12861137]
16. Hill CR, ter Haar GR. Review article: high intensity focused ultrasound--potential for cancer treatment. *Br J Radiol*. 1995; 68:1296–303. [PubMed: 8777589]
17. Kennedy JE. High-intensity focused ultrasound in the treatment of solid tumours. *Nat Rev Cancer*. 2005; 5:321–7. [PubMed: 15776004]
18. ter Haar G, Stratford IJ, Hill CR. Ultrasonic irradiation of mammalian cells in vitro at hyperthermic temperatures. *Br J Radiol*. 1980; 53:784–9. [PubMed: 7437689]
19. Shahmirzadi D, Hou GY, Chen J, Konofagou EE. *Ex Vivo* Characterization of Canine Liver Tissue Viscoelasticity After High-Intensity Focused Ultrasound Ablation (In Press). *Ultrasound Med Biol*. 2013
20. Nandlall SD, Schiffter HA, Vonhoff S, Bazan-Peregrino M, Arora M, Coussios CC. Real-time optical measurement of biologically relevant thermal damage in tissue-mimicking hydrogels containing bovine serum albumin. *International Journal of Hyperthermia*. 2010; 26:456–64. [PubMed: 20569110]
21. Lafon C, Zderic V, Noble ML, Yuen JC, Kaczkowski PJ, Sapozhnikov OA, et al. Gel phantom for use in high-intensity focused ultrasound dosimetry. *Ultrasound in Medicine and Biology*. 2005; 31:1383–9. [PubMed: 16223642]
22. Wu T, Felmlee JP, Greenleaf JF, Riederer SJ, Ehman RL. Assessment of thermal tissue ablation with MR elastography. *Magnetic Resonance in Medicine*. 2001; 45:80–7. [PubMed: 11146489]
23. Chen CC, Miga MI, Galloway RL. Characterization of tracked radiofrequency ablation in phantom. *Med Phys*. 2007; 34:4030–40. [PubMed: 17985649]
24. Divkovic GW, Liebler M, Braun K, Dreyer T, Huber PE, Jenne JW. Thermal properties and changes of acoustic parameters in an egg white phantom during heating and coagulation by high intensity focused ultrasound. *Ultrasound Med Biol*. 2006; 33:981–6. [PubMed: 17434665]
25. Iizuka MN, Sherar MD, Vitkin IA. Optical phantom materials for near infrared laser photocoagulation studies. *Lasers Surg Med*. 1999; 25:159–69. [PubMed: 10455223]
26. Takegami K, Kaneko Y, Watanabe T, Maruyama T, Matsumoto Y, Nagawa H. Polyacrylamide gel containing egg white as new model for irradiation experiments using focused ultrasound. *Ultrasound Med Biol*. 2004; 30:1419–22. [PubMed: 15582242]
27. Maleke C, Konofagou EE. Harmonic motion imaging for focused ultrasound (HMIFU): a fully integrated technique for sonication and monitoring of thermal ablation in tissues. *Phys Med Biol*. 2008; 53:1773–93. [PubMed: 18367802]
28. Hynynen, K. Biophysics and Technology of Ultrasound Hyperthermia. In: Gautherie, M., editor. *Methods of External Hyperthermic Heating*. New York: Springer-Verlag; 1990.

29. Noguera G, Lee WS, Castro-Combs J, Chuck RS, Soltz B, Soltz R, et al. Novel laser-activated solder for sealing corneal wounds. *Invest Ophthalmol Vis Sci*. 2007; 48:1038–42. [PubMed: 17325144]
30. Hui AY, McCarty WJ, Masuda K, Firestein GS, Sah RL. A systems biology approach to synovial joint lubrication in health, injury, and disease. *Wiley Interdiscip Rev Syst Biol Med*. 2012; 4:15–37. [PubMed: 21826801]
31. Maleke C, Konofagou EE. An all-ultrasound-based system for real-time monitoring and sonication of temperature change and ablation. *Conf Proc IEEE Eng Med Biol Soc*. 2006; 1:164–7. [PubMed: 17946794]
32. Maleke, C.; Pernot, M.; Konofagou, EE. A single-element focused transducer method for harmonic motion imaging. *Proc IEEE Ultrasonics Symp*; Rotterdam, Netherlands. 2005. p. 17-20.
33. Maleke C, Pernot M, Konofagou EE. Single-element focused ultrasound transducer method for harmonic motion imaging. *Ultrason Imaging*. 2006; 28:144–58. [PubMed: 17147056]
34. Choi JJ, Wang SG, Tung YS, Morrison B, Konofagou EE. Molecules of Various Pharmacologically-Relevant Sizes Can Cross the Ultrasound-Induced Blood-Brain Barrier Opening in Vivo. *Ultrasound Med Biol*. 2010; 36:58–67. [PubMed: 19900750]
35. Hou GY, Marquet F, Wang ST, Konofagou EE. Multi-parametric monitoring and assessment of high-intensity focused ultrasound (HIFU) boiling by harmonic motion imaging for focused ultrasound (HMIFU): an ex vivo feasibility study. *Phys Med Biol*. 2014; 59
36. Tan AR, Dong EY, Ateshian GA, Hung CT. Response of engineered cartilage to mechanical insult depends on construct maturity. *Osteoarthritis Cartilage*. 2010; 18:1577–85. [PubMed: 20851200]
37. Kelly T-AN, Roach BL, Weidner ZD, Mackenzie-Smith CR, O’Connell GD, Lima EG, et al. Tissue-engineered articular cartilage exhibits tension–compression nonlinearity reminiscent of the native cartilage. *Journal of Biomechanics*. 2013; 46:1784–91. [PubMed: 23791084]
38. Farndale RW, Sayers CA, Barrett AJ. A direct spectrophotometric microassay for sulfated glycosaminoglycans in cartilage cultures. *Connect Tissue Res*. 1982; 9:247–8. [PubMed: 6215207]
39. Wang S, Mahesh SP, Liu J, Geist C, Zderic V. Focused ultrasound facilitated thermo-chemotherapy for targeted retinoblastoma treatment: a modeling study. *Exp Eye Res*. 2012; 100:17–25. [PubMed: 22564972]
40. Lima EG, Bian L, Ng KW, Mauck RL, Byers BA, Tuan RS, et al. The beneficial effect of delayed compressive loading on tissue-engineered cartilage constructs cultured with TGF-beta3. *Osteoarthritis and cartilage / OARS, Osteoarthritis Research Society*. 2007; 15:1025–33.
41. Good CR, Shindle MK, Griffith MH, Wanich T, Warren RF. Effect of radiofrequency energy on glenohumeral fluid temperature during shoulder arthroscopy. *J Bone Joint Surg Am*. 2009; 91:429–34. [PubMed: 19181988]
42. Protsenko DE, Zemek A, Wong BJ. Temperature dependent change in equilibrium elastic modulus after thermally induced stress relaxation in porcine septal cartilage. *Lasers Surg Med*. 2008; 40:202–10. [PubMed: 18366085]
43. Shellock FG. Radiofrequency energy induced heating of bovine articular cartilage: comparison between temperature-controlled, monopolar, and bipolar systems. *Knee Surg Sports Traumatol Arthrosc*. 2001; 9:392–7. [PubMed: 11734879]
44. Yasura K, Nakagawa Y, Kobayashi M, Kuroki H, Nakamura T. Mechanical and biochemical effect of monopolar radiofrequency energy on human articular cartilage: an in vitro study. *Am J Sports Med*. 2006; 34:1322–7. [PubMed: 16685093]
45. Karam AM, Protsenko DE, Li C, Wright R, Liaw LH, Milner TE, et al. Long-term viability and mechanical behavior following laser cartilage reshaping. *Arch Facial Plast Surg*. 2006; 8:105–16. [PubMed: 16549737]

Highlights

- High Intensity Focused Ultrasound (HIFU) may be appropriated for controlled heating of tissue volumes, which could be used to alter tissue properties of engineered grafts during *in vitro* culture.
- HIFU treatment of gel phantoms with incorporated egg white showed a decrease in permeability and increase in stiffness in the affected regions.
- Cell death from heating remained localized to the thermally affected region over time.
- It is expected that this heating technology may have many applications across many tissue types in the field of tissue engineering.

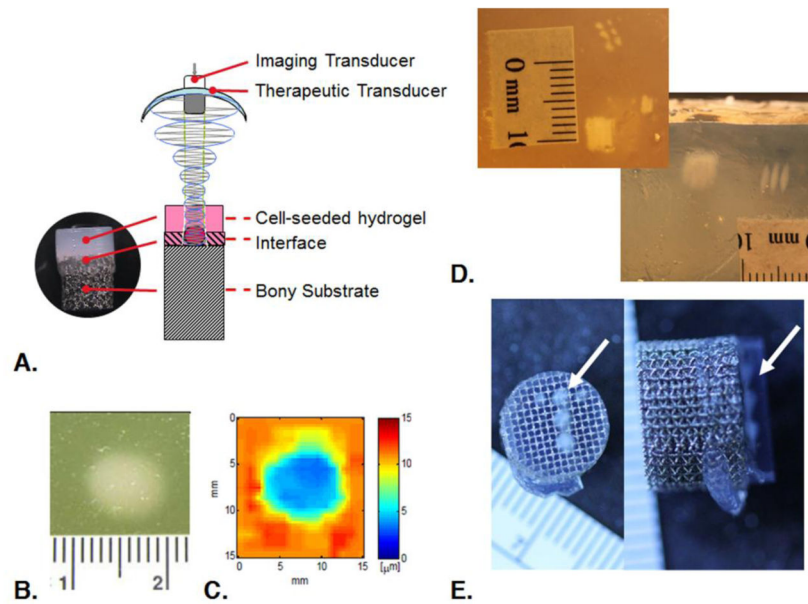


Figure 1.

(A) Schematic of HIFU treatment of osteochondral construct. The two-transducer system is attached to a computer-controlled positioner. (B–C) Circular thermally affected region induced in an egg white gel by HIFU with a 25 s duration in the center and 10 s duration in the surrounding ring (~6 MPa peak *in situ* positive pressure), which was then mapped using HMI using a rastered step size of 1 mm across a $15 \times 15 \text{ mm}^2$ region (peak-positive pressure of 1.98 MPa, 500 ms/point duration). The circular egg-white pattern indicated that the thermally affected region was three times stiffer than the surrounding gel. (B) Gross Image and (C) HMI map of HIFU-induced thermally affected region. Color bar shows oscillatory displacement in μm (lower displacements correspond to stiffer regions). (D) Thermally affected region patterns beneath the surface of agarose-egg white gel (Top and Side views). (E) Osteochondral constructs (Top and Side views) displaying thermally affected regions created at different powers. Arrows indicate 11.6 W total acoustic power for 20 s. Scale bars indicate millimeters.

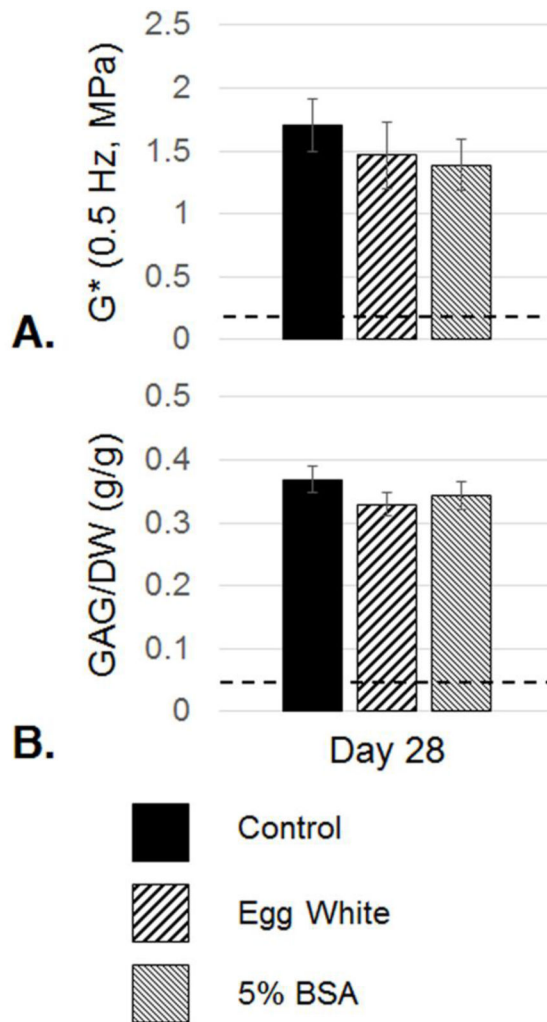


Figure 2. Unimpeded growth in constructs with incorporated albumin. (A) G^* at 0.5 Hz ($n=6$ per group) and (B) GAG content per dry weight ($n=4-6$ per group) of chondrocyte-seeded agarose constructs: control, and egg white or BSA supplemented on day 28. Error bars show 95% CI. The dashed line represents the mean of day 0 values across groups ($n=3-4$ per group).

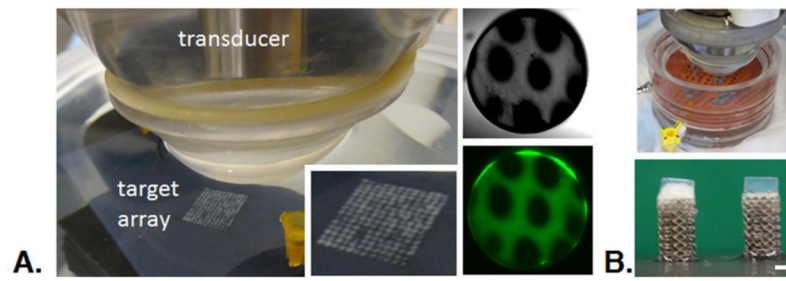


Figure 3.

(A) Setup showing HIFU-induced array of thermally affected regions (left, inset shows array magnified). Fluorescein-dextran soaked construct viewed under transmitted light to visualize thermally affected sites (top-right) and fluorescence (bottom-right) showing dextran exclusion from those same sites. (B) Top: Sterile ultrasound chamber; Bottom: Osteochondral constructs showing HIFU-induced egg white lesion (left) and no treatment (right). Scale bar: 1 mm.

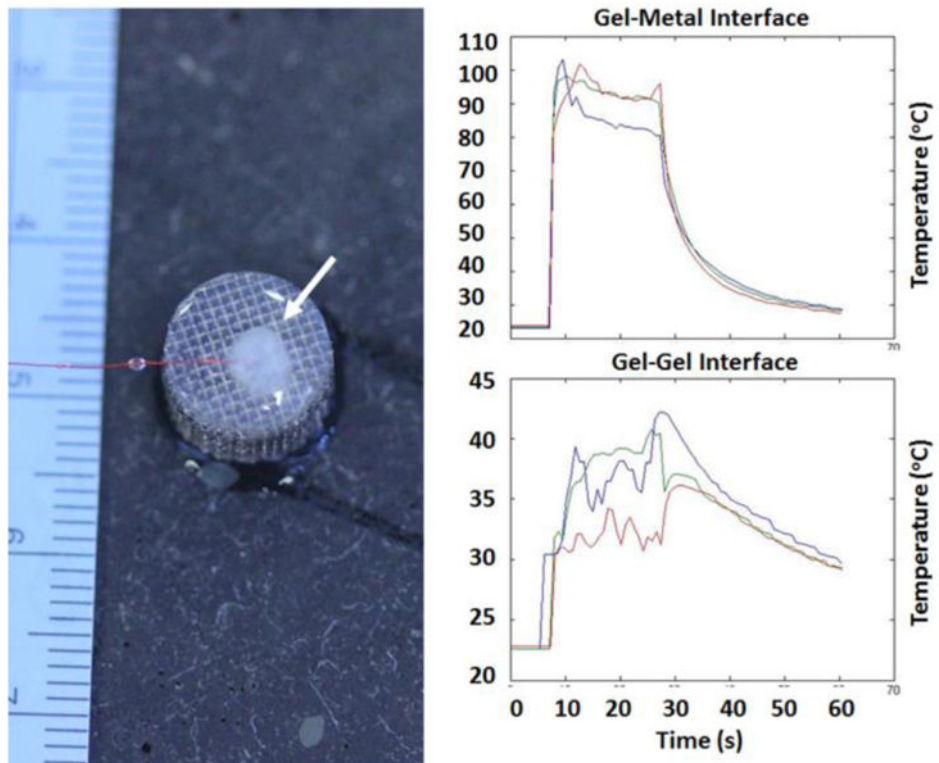


Figure 4. Enhanced temperature elevations with incorporated base. Left: Gross image of osteochondral construct with HIFU-induced denaturation region with thermocouple inserted (Arrow). Scale bar indicates millimeters. Temperature readings across 60 s containing 20 s of 11.6 W total acoustic power excitation at the gel-metal interface (Top-right) and between layered gels (Bottom-right).

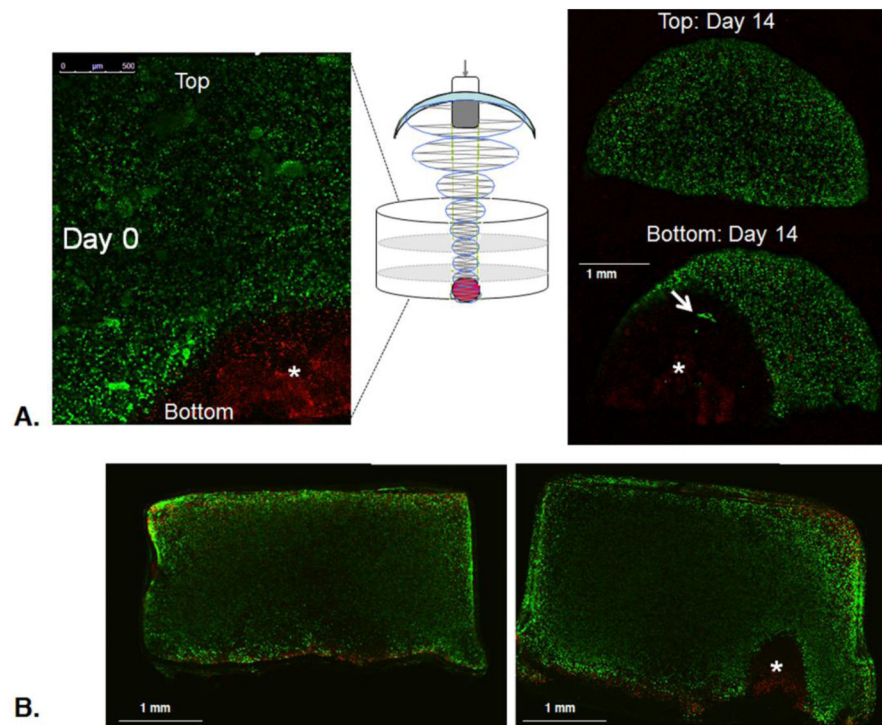


Figure 5. Cell viability effects remain localized over time. (A) Representative Live/Dead staining of the axial cross-section immediately after HIFU (Day 0, left), and an upper and lower (HIFU treated) transverse plane 14 days post-HIFU (Day 14, right). Both images show localized cell death due to ultrasound treatment. Asterisks indicate HIFU treated zone. Arrow indicates area of possible cell recovery. (B) Live/Dead images of removed gel regions of $\varnothing 4$ mm osteochondral constructs: control (left) and HIFU-treated (right) 28 days after treatment date.